

# Statistical diagnostics of injected continuous wave signals for analysis of candidates from directed searches

Sam Imperato

*Northwestern University, Evanston, IL 60201, USA  
Università di Roma ‘La Sapienza’, I-00185 Roma, Italy*

Ornella Piccinni

*INFN, Sezione di Roma, I-00185 Roma, Italy  
Università di Roma ‘La Sapienza’, I-00185 Roma, Italy*

(Dated: November 11, 2021)

The purpose of the study was to test a new follow-up procedure for potential candidates of continuous wave (CW) signals injected into LIGO, Virgo or KAGRA data. The eventual recovery of the signal is assessed using a semi-coherent method based on the well known 5-vector method, typically used for known pulsar searches. The chief goal of this work is determining the degree away that the estimated parameters can be from the correct parameters while still being able to recover the signal. The methodology included injecting signals with a chosen frequency, and creating a grid for each injected signal over a range of frequencies near the injection and a range of coherence lengths. In addition this study used grids which kept the coherence length constant and set to an optimal value based on the frequency injected, while the grids were created over the parameters of frequency, spin-down and sky location. For both types of grid, the data was corrected and the five-vector method was applied to both the corrected and not-corrected data. To determine the significance of an injection from that point in parameter space, the critical ratio (CR) and signal-to-noise ratio (SNR) were compared for the corrected and not-corrected data. We find that for the majority of cases, the signal can be recovered when the parameters are anywhere within the natural grid size. In the frequency versus coherence time grids, the signal can be found only in the frequencies very close to the injected frequency, since a much wider frequency range is probed if compared to the previous cases. These findings will be applied to analysis study of signal candidates from a directed search for continuous gravitational waves.

## I. INTRODUCTION

Gravitational waves have so far been detected from mergers of binary black holes, binary neutron stars, and black hole neutron star binaries. In addition to detection of compact binary coalescence (CBC), other astrophysical sources are expected to produce different types of detectable gravitational waves. An important class of gravitational wave signals is continuous gravitational waves (CW). CW can be produced by a variety of sources, but the primary source is expected to be spinning asymmetric neutron stars, including pulsars. Gravitational waves have previously been observed indirectly and directly from neutron star binaries, but they have yet to be detected from isolated neutron stars. In fact no CW observations have been made to date.

While no CW observations have yet been made, there are different types of searches looking for these signals. In the isolated neutron star case, these searches can be divided into targeted, narrow-band, directed, and all-sky. The targeted and narrow-band searches assume all parameters of the neutron star are known or, in the case of the narrow-band, the phase evolution of the signal model is relaxed and typically is fully coherent, where a matched filter is applied to the full parameter space covered, and the full dataset is used in the analysis. For directed searches, only the sky location is fixed, while for all-sky searches no parameters are known or assumed. A

directed search can be compared to the case when astronomers point a detector at an interesting location, for example the center of the milky way galaxy, where a huge number of sources is expected to be present. In this work, we principally assume that the uncertainty of the sky locations is negligible, as for the case of the directed search.

Data analysis methods are used to find the signal in the LIGO, Virgo, or KAGRA detectors. The signal analysis procedure for CWs has some similarities to the method applied to mergers, however, CW signals have unique challenges. The merger signals that have been detected numerous times are on the order of seconds to minutes, while the expected CW signals can last for months and even years. The CBC signals are additionally orders of magnitude louder than CW signals. The typical matched filter detection method for CBC signals is used in fully coherent searches for CW signals, but because of the length of CW signals, semi-coherent methods have been developed when the parameter space to investigate becomes too large, as used in this study.

## II. FIVE-VECTOR METHOD

One of the methods used to look for continuous gravitational wave signals is the five-vector method [1] The five-vector method is named for its representation of the data using vectors of 5 components, based on the signal

intrinsic angular frequency ( $\omega_0$ ), and Earth's sidereal angular frequency ( $\Omega_0$ ). The 5 frequencies used in the five-vector method are ( $\omega_0 - 2\Omega_0, \omega_0 - \Omega_0, \omega_0, \omega_0 + \Omega_0, \omega_0 + 2\Omega_0$ ).

The five-vector method fully describes the signal using just the five Fourier components. The signal template is constructed and is matched to the actual data received from the gravitational wave detector.

It is also possible to represent the data as a 5-vector as in Eq. 2. In this case 5-vector of the data ( $\mathbf{X}$ ) will contain both the noise 5-vector ( $\mathbf{N}$ ) plus an eventual signal ( $\mathbf{S}$ ).

### A. The signal five-vector

Eq. 1 is the signal five-vector, where  $H_0$  is the maximum amplitude of a signal, and  $\Phi_0$  is the phase at time  $t_0$ . [2]

$$\mathbf{S} = H_0 e^{j\Phi_0} (H_+ \mathbf{A}^+ + H_\times \mathbf{A}^\times) \quad (1)$$

The signal five-vector is constructed using the plus and cross amplitudes,  $H^+$  and  $H^\times$ . These amplitudes depend on the polarization parameters,  $\eta$  and  $\psi$ .  $\eta$  is the ratio of the semi-minor axis to the semi-major axis of the polarization ellipse, and  $\psi$  is the polarization angle.

$$H^+ = \frac{\cos 2\psi - j\eta \sin 2\psi}{\sqrt{1 + \eta^2}}$$

$$H^\times = \frac{\sin 2\psi + j\eta \cos 2\psi}{\sqrt{1 + \eta^2}}$$

$\mathbf{A}^+$  and  $\mathbf{A}^\times$  describe the detector response as a function of time.

### B. The data five-vector

The data five-vector is the signal five-vector ( $\mathbf{N}$ ) with the addition of the noise five-vector.

$$\mathbf{X} = \mathbf{S} + \mathbf{N} \quad (2)$$

$$\mathbf{X} = H_0 e^{j\Phi_0} (H_+ \mathbf{A}^+ + H_\times \mathbf{A}^\times) + \mathbf{N} \quad (3)$$

### C. Signal statistics

From the use of the five-vector method, different statistics are used to assess the significance of the signal compared to the data. The two focused on in this work are the CR and the SNR. The CR is calculated as  $\frac{S - \mu_{noise}}{\sigma_{noise}}$ , and the SNR is  $\frac{S}{\sigma_{noise}}$ .  $S$  is the statistic defined in [1]. Here, CR is the main metric used to determine whether a signal is present in the gravitational wave detector data.

### D. The continuous wave signal

The source of the CWs, the neutron star, is described by different parameters that change the CW being emitted. These include the intrinsic source parameters, which consists of the frequency of its spin, the degree of asymmetry or the ellipticity which would change the amplitude of the signal, in addition to its distance from Earth, and spin-down, which is the rate of its decrease in frequency. In addition to the intrinsic source parameters, there are other parameters that also have an effect on the CW signal. Typically, spin-down is a negative non zero first derivative of the frequency of the pulsar, but it can be positive in certain cases. One possible scenario resulting in an increase in the frequency of a neutron stars spin is mass accreting onto the pulsar, as in a low-mass x-ray binary system. Upper limits on the strength of spin-down have been calculated based on astronomical observations on pulsars where their spins have gradually slowed down, and in this study it is assumed that the maximum spin-down is  $-10^{-8}$ . In addition, spin-up, where the spin of the neutron star is increasing over time, is explored in this study on the order of  $+10^{-12}$ . This is a lower magnitude than the negative spin-down, but is in the positive direction. Assuming the astronomically observed spin-down is all attributed to gravitational waves being emitted, as it would decrease the angular momentum of the neutron star, the maximum gravitational waves that would be radiated from the pulsar can be calculated. Other important parameters that describe the system include the polarization of the CW signal and the location of Earth in its orbit. The polarisation is a weighted combination of the cross and plus polarisation. This is due to the angle of the pulsar's spin with respect to Earth. Extrinsic parameters such as location of Earth in its orbit, among other parameters, is particularly important when removing modulations from the data.

## III. METHODS

This project aimed to explore parameter space around injected signals, with the goal of mimicking the candidate follow-up process that would take place after CW signal candidates would be identified from a directed or all-sky search. The parameters looked into in this study were the frequency of the source, the first order spin-down of the source, the coherence length used in the analysis, and the location of the signal in the sky.

The general process for determining the significance of whether a signal could be uncovered in a specific location in the data included four steps. The first was to extract a frequency band in the data from the gravitational wave detector. A signal is then injected whose frequency lies in the same frequency band that has been extracted. In this study we focused on data from the LIGO Hanford gravitational wave detector from the third observing run, O3. We use the data in a format called band-sampled-data, or

BSD. [2] In this format, each BSD file is a complex time series, covering 1 month of data and a 10Hz frequency band. From this, the power spectrum in the frequency domain can be computed. Because at this point in the analysis procedure for a signal candidate from a directed search the location of the signal frequency would already be known with some uncertainty, only a small frequency band is needed to be extracted from the GW detector data. This uncertainty is fully covered by a single sky bin if the coherence time used is sufficiently short, so it is negligible. Typically the size of this frequency band was chosen to be about 0.4 Hz. This size was small enough to be able to run the codes in a reasonable amount of time and not take too much storage, but was large enough to fully contain the signal.

Next the signal must be injected into the extracted GW detector data. When the actual signal candidates are being explored no injections would be used, but in this study they are utilized for a test purpose. The parameters for the injection signal were chosen to cover a wide range of possible source parameters and then the signal is added to the data.

For the five-vector method to be applied, the data must be corrected to remove the Doppler shift and other modulations of the signal. Other than the spin-down, the frequency of the pulsar that is emitted from the source is monochromatic. However, the signal that reaches the gravitational wave detector on Earth is not monochromatic. This is because of modulations in the signal due to Earth's rotation and revolution, gravitational redshift, and other factors that change the shape of the signal, and the detector response.

The two main methods of data correction are called resampling and heterodyne. In this work the heterodyne method is used, and it is implemented by multiplying the BSD data by an exponential factor  $e^{-i\phi}$ , where  $\phi$  is the phase associated to the frequency of the source and its modulations.

The removal of the modulations is necessary when using the five-vector method to find signals in the data as the method looks for frequency peaks at certain values. If the modulations were to not be removed, the five-vector pattern would not arise as it is only present when the sidereal effect is the only modulation left. When the data is modulated, these peaks are non-existent or in incorrect locations. However the uncorrected data can still be useful in analysis, and in this study the five-vector method is applied to both the corrected and uncorrected data, so the difference between the two can be used to determine if the method is picking up an actual signal or just a pattern of noise in the data.

Next, grids over the parameter space in the vicinity of the injected signals parameters are created, and the parameters of each point on the grid were used to correct the data. The correction is where the Doppler effect, the Einstein effect and the spindown are removed using a procedure that oversamples the data which only leaves behind the monochromatic GW signal with just modula-

tion from the detector response.

The five-vector method was then applied to both the corrected and the uncorrected data. This process aims to mimic the situation in which the origin of a candidate is being assessed, assuming that the parameters inferred of the candidate can be slightly incorrect. The parameters changed within the grids are the frequency of the source, the first order spin-down, and the sky location of the source. The size of these grids is set by the coherence length, which is additionally changed in some of the grids. Using the five-vector method calculates different metrics about the strength of the signal compared to the strength of the noise, including the CR and the SNR. These metrics are calculated for every point on the grid for both the corrected and uncorrected data, to determine where in the parameter space near the injected signals the signals can be uncovered.

TABLE I: Injections for changing frequency and coherence length

$f_0$ [Hz]	$\dot{f}_0$ [Hz/s]	$T_{FFT}$ [s]	RA	Dec
102	$-1 \times 10^{-8}$	$10^4$ to $10^7$	33.4366	178.3726
350	$-1 \times 10^{-8}$	$10^4$ to $10^7$	33.4366	178.3726
500	$-1 \times 10^{-8}$	$10^4$ to $10^7$	33.4366	178.3726
550	$-1 \times 10^{-8}$	$10^4$ to $10^7$	33.4366	178.3726
850	$-1 \times 10^{-8}$	$10^4$ to $10^7$	33.4366	178.3726
1000	$-1 \times 10^{-8}$	$10^4$ to $10^7$	33.4366	178.3726

#### A. Set up of frequency and coherence length grids

Two different classes of grids around parameter space were used in this study, with first being grids over different frequencies and different coherence lengths ( $T_{FFT}$ ). The sky position and the polarization parameters were those of the hardware injection "pulsar 3", while the frequency was the only injection parameter changed in this section of the project. The coherence length or the amount of the data in the time series is analyzed in one batch to search for the signal was not fixed and was instead changed from a range of  $10^4$  to  $10^7$  seconds. The lower limit of  $10^4$  is less than the 86,000 s necessary for the five-vector feature to be visible, so no significant results are expected to be found at that magnitude. The chosen frequency injected is far away from the actual frequency of the hardware injection, and the range of values used to correct the signal were set at  $\pm 0.002$  Hz away from the chosen injected frequency. Table 1 is the injections used in this part of the study. Then a grid was created over these frequency and coherence length values in order to cover every point in the parameter space within these bounds. The spacing for the frequency was 0.0004 Hz apart, and the coherence lengths were an order of magnitude apart. The data was then corrected at

each point on the grid, and the five-vector method was applied on both the corrected and uncorrected data for every point, returning metrics describing the strength of the signal in that location in parameter space. The CR was then normalized by the numbers of chunks of data used. Then, after this correction, the CRs for the different coherence lengths could be compared.

### B. Natural coherence length and grid size

The other type of grid used in this study kept a constant coherence length and was instead over different parameters of the system, including frequency, spin-down and sky location of the pulsar. This type also differs from the previous, because the bounds of the grid were not set to be +/- 0.002 Hz away from the injected signal, but instead the grid size was based on the optimal coherence length for a given frequency. The optimal coherence length for giving frequency was based on a few different parameters including the speed of light  $c$ , the frequency being searched, the radius of Earth's orbit,  $R_{orb}$ , and Earth's orbital angular velocity,  $\Omega_{orb}$ . The Eq. used in this study to calculate the optimal coherence length is as follows.

$$T_{FFT} = \sqrt{\frac{16c}{2f_{max}\Omega_{orb}R_{orb}}} \quad (4)$$

The grid bounds are the uncertainty of the location of the signal. In this study only one coarse grid point, defined as one bin, is used, and the bounds of the one coarse grid become the bounds of the grid that will later be refined.

The typical coherence length for all frequencies covered in the BSD in a directed search is always less than one sidereal day, which is approximately 86400 seconds long. [3] When the coherence length is less than one sidereal day, the five-vector pattern is not visible, so the grid must be refined to be able to use a longer coherence length.

The coherence length used in the search,  $T_{search}$ , defines a frequency bin of  $1/T_{search}$ . [4] The uncertainties of a directed search candidate in frequency is equal to the frequency bin size. The same is true for the spin-down, in that the uncertainty is equal to the spin-down bin which is also dependent on  $T_{search}$ . In order for the actual location of the injected signal to always be centered in one bin, when this number was even, 1 was added to it.

In addition to natural coherence lengths, the range of the grid bounds were also calculated based on an ideal range. The first type of natural grid was over frequency and spin-down. Each grid had a different pair of frequency and spin-down used in the injected signal, where every frequency was ran twice with both a spin-down of  $-10^{-8}$  and a spin-up of  $+10^{-12}$ . Within each grid, the injection signal remained the same, but the parameters used to correct and analyze the signal were changed for each point. The parameters of each injection used for

these types of grids are listed in table 2. The grids were over a range of frequencies and spin-downs for correcting and analyzing the data with the injection. The natural bounds for frequency were calculated with Eq. 5.

$$\delta f = \frac{1}{T_{FFT}} \quad (5)$$

The bounds for the grid over spin-down are calculated using Eq. 6.

$$\delta \dot{f} = \frac{\delta f}{T_{obs}K_f} \quad (6)$$

Where  $T_{obs}$  is the observing time of the signal, and  $K_f$  is a constant set to 2. The spin-down bin location was calculated to place the injected signal in the center, as with the frequency bin.

Using the lists of points for the frequency and spin-down parameters, grids were constructed over these two parameters.

TABLE II: Parameters of the injections for the grids with changing frequency and spin-down.

$f_0$ [Hz]	$\dot{f}_0$ [Hz/s]	$T_{search}$ [s]	RA	Dec
217	$-1 \times 10^{-8}$	19492	33.4366	178.3726
217	$+1 \times 10^{-12}$	19492	33.4366	178.3726
500	$-1 \times 10^{-8}$	12842	33.4366	178.3726
500	$+1 \times 10^{-12}$	12842	33.4366	178.3726
531	$-1 \times 10^{-8}$	12461	33.4366	178.3726
531	$+1 \times 10^{-12}$	12461	33.4366	178.3726
852	$-1 \times 10^{-8}$	9837.6	33.4366	178.3726
852	$+1 \times 10^{-12}$	9837.6	33.4366	178.3726

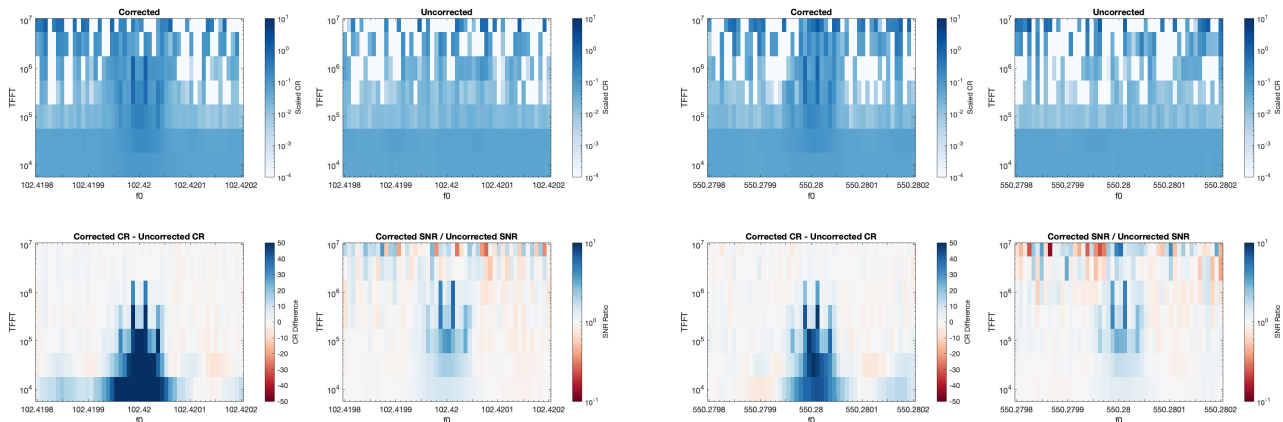
The other type of natural grid was over different locations in the sky. In this case, the frequency and spin-down were kept constant for each injection, so the frequency of each injected signal was  $f_0 = 350$  Hz and the spin-down of each injected signal was  $\dot{f}_0 = -10^{-8}$  Hz/s, and the same ideal coherence length calculation was used. Instead, the sky location was changed for each injection, and was the parameter changed over the grid for the correction and analysis. The parameters of the injections used for these sky location grids are listed in table 3.

For the first sky location parameter, the ecliptic longitude  $\lambda$ , the coarse grid size was calculated with

$$\delta \lambda = \frac{c}{f_0 \Omega_{orb} R_{orb} T_{search} \cos \beta} \quad (7)$$

And for the second sky location parameter, the ecliptic latitude  $\beta$ , the coarse grid size was calculated using the similar formula as the previous, listed below.

$$\delta \beta = \frac{c}{f_0 \Omega_{orb} R_{orb} T_{search} \sin \beta} \quad (8)$$



(a) A grid over frequency and coherence length, with the frequency of the source injection of 102.42 Hz.

(b) A grid over frequency and coherence length, with the frequency of the source injection of 550.28 Hz.

FIG. 1: For both panels of the above figure, the 4 plots represent the same metric. The top left plots are the CR for each point on the grid when the data was corrected using the parameters of that point on the grid, and five-vector method was applied to the corrected data. The top right plots are the CR for when the five-vector method was applied on the uncorrected data using the parameters of the point on the grid. The bottom left plot is CR for the uncorrected data subtracted from the CR for the corrected data, and the bottom right plot is the SNR for the corrected data divided by the SNR on the uncorrected data. For both plots on the bottom row, a blue grid point indicates the CR or SNR was higher for the corrected data, a white point is that the two were similar, and a point in red would be a higher value for the uncorrected data. This comparison is important in finding a signal, and a higher CR and SNR for corrected data indicates a signal was found at that point in parameter space.

The process for creating the grids over the locations in the sky were the same as the frequency and spin-down grids but using the sky location parameters instead of frequency and spin-down.

TABLE III: Injections for changing sky location

$f_0$ [Hz]	$\dot{f}_0$ [Hz/s]	$T_{search}$ [s]	RA	Dec
350	$-1 \times 10^{-8}$	15349	80.5508,	-14.2919
350	$-1 \times 10^{-8}$	15349	-71.9237	49.7799

For both types of grid, the grids over frequency and coherence length and the natural grids over different after physical parameters of the source, each point on the grid is corrected to remove the modulations, and for both the corrected and uncorrected data the five-vector method is applied and the CR and SNR are calculated.

## IV. RESULTS

### A. Grids over frequency and coherence length

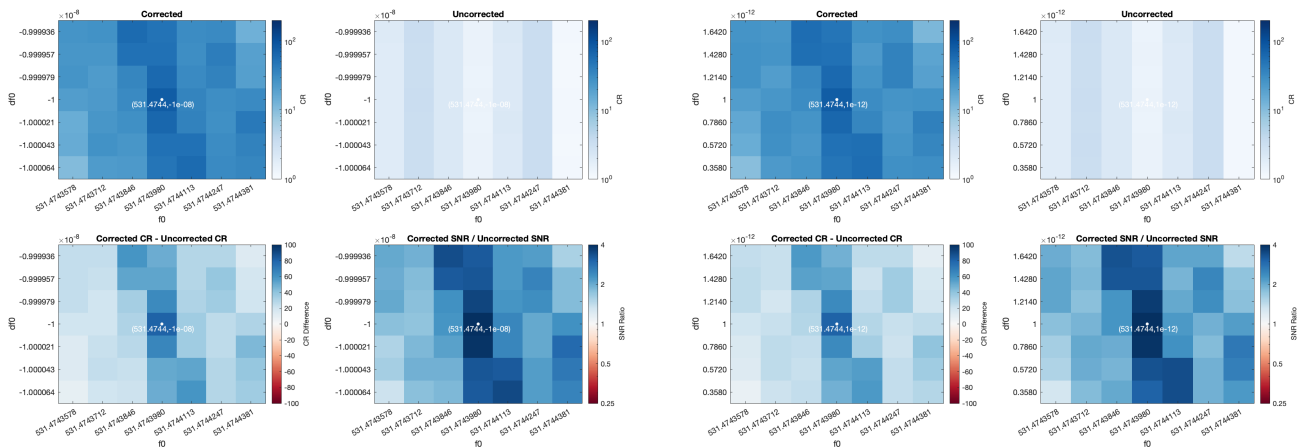
The first type of grid ran in this study was created using different frequency injections but with all other parameters held constant. For each injection, the data was corrected and analyzed using the five-vector method over

a grid of different frequencies in the vicinity of the injection and different coherence length values in the range of  $10^4$  s to  $10^7$  s.

The results of the CR and the SNR can then be compared for the corrected and uncorrected cases to see whether there is a signal present in the data. When the corrected data has a higher CR or SNR than the uncorrected data, the significance of the candidate when we correct the data has increased. This does not give the certainty of a detection, however. If the uncorrected data has a higher or too similar CR or SNR to the corrected data, the five-vector method is only finding noise and does not find an actual signal.

Different coherence lengths are used in these grids, so the CR must be scaled before it can be compared between different coherence lengths. To scale the CR, the full length of time is divided by the coherence length used. Then, the CR is divided by this value.

Looking at these grids, in figure 1 a clear pattern can be seen in the data. For all of the frequency injections used and for each grid, there is a distinct pattern of four peaks in largest corrected CR and SNR compared to corresponding uncorrected data. These peaks are on either side of the injected frequency value. For the middle coherence lengths approximately between  $10^5$  s and  $10^6$  s the highest CR is not at the injected value but at slightly above and slightly below it, giving a characteristic line pattern within the data. This pattern in the grid is clear



(a) A grid over frequency and spin-down, with the frequency of the source injection of 531.4744 Hz and the spin-down of the injected source of  $-10^{-8}$  Hz/s. (b) A grid over frequency and spin-down, with the frequency of the source injection of 531.4744 Hz and the spin-down of the injected source of  $+10^{-12}$  Hz/s.

FIG. 2: Panel a) and b) are grids over frequency and spin-down, both with the frequency of the injected source of 531.4744 Hz. However the source injected in panel a) had a spin-down of  $-10^{-8}$  Hz/s, while the source injected in panel b) had a spin-up of  $+10^{-12}$  Hz/s. The layout of sub-grids remains the same as in figure 1. For both spin-down values for this particular frequency, every point on the grid had a higher CR and SNR for the corrected data than the uncorrected data. This indicates that the signal was able to be found from each point on the grid. Nevertheless, some points have a higher CR and SNR ratio than others. There is a band down the middle of the comparison grids for both the spin-down and spin-up cases with the highest CR and SNR differences, starting at the top left of center and ending on the bottom right of center. The maximum CR ratio and SNR difference lies at the center of the grid where the injection is located. This type of grid could be of additional use in determining if a signal had an astrophysical origin, based on the existence of the band.

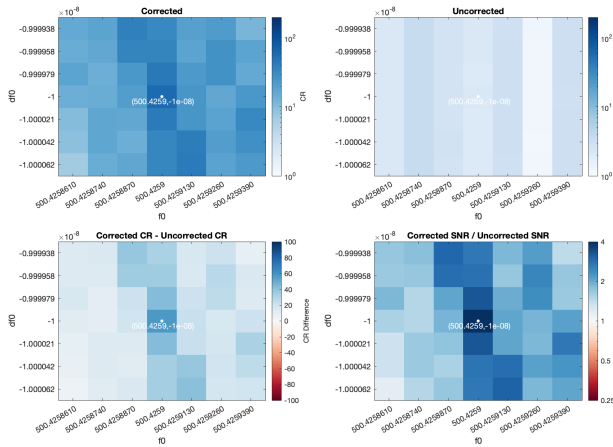
over the entire frequency range tested from 100 to 1800 Hz, in addition to being visible in both metrics, in both the CR grids and the grids colored by SNR. However it must be noted that this was on a small amount of injections, and with the polarization parameters unchanged. More analysis must be done to determine if this pattern is truly ubiquitous.

## B. Grids over frequency and spin-down

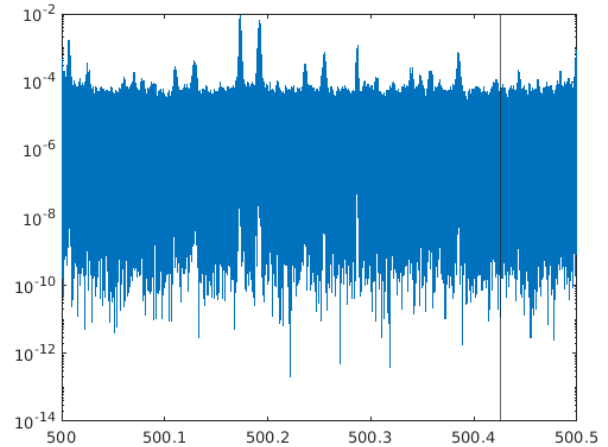
The frequency and spin-down grids are each for an injection with a different source frequency or spin-down value. For these grids the x axis is the different frequency values used to correct and analyze the data and the y-axis values are the different spin-down values used to correct an analyzed data. Each square on this grid was used to correct and analyze the data using the given frequency and spin-down values. The actual values of the injection signal are the center of the grid, and labelled in white. The source injection values are also used to correct an analyzed the data for that point while the other points on the grid were correcting and analyzing the data using intentionally incorrect parameters, to see how well the signal could be recovered even with errors in the parameters estimated. This shows how far away from the actual

injection point the signal can be seen, and also whether there were any biases in regions where the signal was given a higher significance than the actual location of the signal. Another purpose behind these types of grids was to find out if further refining these grids beyond the coarse grid bounds aided in the determination if a candidate had an astrophysical source and where exactly the source was in parameter space.

Figure 2 includes two different grids for the same frequency injection value of 530 Hz. Figure 2a is for a spin-down of  $-1 \times 10^{-8}$  Hz/s, while figure 2b is for  $+1 \times 10^{-12}$  Hz/s.  $-1 \times 10^{-8}$  Hz/s is the maximum magnitude spin-down that is expected based on astronomical observations of pulsars. The maximum spin-up used in this study is  $+1 \times 10^{-12}$  Hz/s. Both panels have a similar pattern for both the positive and negative spin-down cases. This pattern follows a negative slope from to the left of the center at the top of the grid to the right of the center at the bottom of the grid for where the highest CR and SNR difference is for the corrected versus the uncorrected cases. The spin-up case had the exact same pattern, which initially was unexpected, because the pattern was expected to follow a positive slope starting from the bottom left to the top right of the grid. Instead it follows the same pattern as the negative spin-down case. If the maximum spin-up magnitude used was higher than  $+1 \times 10^{-12}$  Hz/s, it is possible that this pattern would differ from the



(a) Grid for a source injection with frequency of 500 Hz, and spin-down of  $-10^{-8}$  Hz/s



(b) Power spectrum of the 500.0-500.5 Hz band.

FIG. 3: Frequency and spin-down grid for a frequency injection in a band with above average noise. The difference between the corrected and uncorrected case is not as strong as with signals in clear bands, but the signal is still clearly able to be recovered.

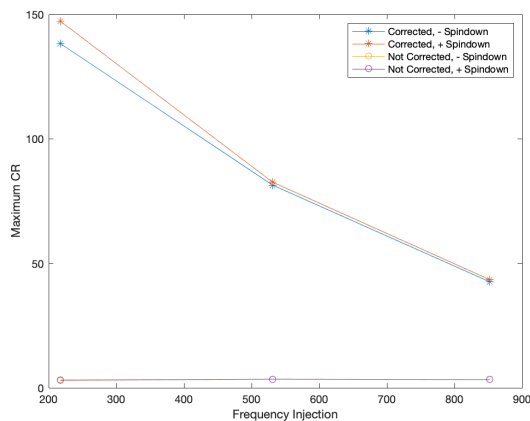


FIG. 4: The maximum CR for each frequency injection, for both types of spin-down and for the corrected and uncorrected data. The uncorrected data is approximately constant, and extremely low, over the entire frequency range. For the corrected data the maximum critical ratio decreases as frequency increases.

For both corrected and uncorrected, there is no significant difference between spin-up and spin-down cases.

negative spin-down case, however the maximum spin-up magnitude is too low for this pattern to be broken.

Multiple frequency injections were used to create different grids with using both spin-down values of  $-1 \times 10^{-8}$  Hz/s and  $+1 \times 10^{-12}$  Hz/s for each frequency. In total, 6 different pairs of spin-up and spin-down grids over different frequency injection values like figure 2 were used. The same process with applying the five-vector

method to the corrected and uncorrected data for each one on the grid for both the spin-up and spin-down grids.

Figure 3 shows the maximum CR for the corrected and uncorrected cases for both the positive spin-up and the negative spin-down injections. For the corrected case, the spin-up and spin-down cases differ very little and are approximately the same for their respective frequency injections. However, the maximum scaled CR decreases as the frequency using the injection increases, but this appears to level off around 800 Hz. for the uncorrected data, the spin-up and spin-down cases again differ very little, the maximum scaled CR is approximately constant throughout the entire range of the frequency value injected into the data. In addition, for each frequency injection value the corrected maximum scale CR is higher than the respective maximum scaled CR for the uncorrected cases.

The comparison of the max CR for different frequency injections, figure 3, is only for frequency injections in clean areas of the gravitational wave detector BSD data. Two tests were done with signals injected with a frequency in visually polluted frequency bands. Figure 4 is of grids for a frequency in an area of the band with a somewhat high amount of noise at 500 Hz, and the right panel of the figure is of the uncorrected power spectrum the signal was later injected into. In this case, the analysis yielded the same results as the injections in relatively low noise bands. A test was also done in the heavily polluted 1000 Hz band, but the signal was not able to be recovered.

## V. DISCUSSIONS & CONCLUSION

The preliminary purpose of this study was to explore parameter space around the vicinity of injected CW signals. This is the groundwork for a future study which will apply these processes to the actual signal candidates from a directed search in the LIGO O3 data. However, even these preliminary results can be important before taking the next steps.

For the frequency vs spin-down grids, there was a clear pattern with a diagonal band with negative slope from the top left of center to the bottom right of center on the grids, with the region of highest CR and SNR difference for the corrected data versus the uncorrected data. This pattern could be a clue of the presence of an astrophysical signal, as it is unlikely to happen randomly and appears for all grids of this type used, which however notably did not cover different polarization parameters. This pattern was even visible for the SNR ratio grid for a signal injected into a moderately polluted frequency band.

For the grids over frequency and coherence length, using the fixed polarization parameters, there is a distinct pattern in every single grid with 4 lines of high CR and SNR difference, with 2 lines in the center being the strongest. These lines surprisingly are not on the injected location but actually are 2 points to the left and to the right of the actual injected location. For the y axis, the coherence length maximum CR and SNR difference values are between the order of  $10^5$  s and  $10^6$  s. There is also a high CR for all points near to the injected frequency for the shortest coherence lengths. These findings can be important in studying whether a signal candidates is of astrophysical origin, as the grids on injected signals had particular pattern that is unlikely to be created by random noise and could be matched to grids of signal candidates.

## VI. FUTURE WORK

Multiple aspects of this study could be further clarified and explored in future work.

All of the analysis in the study was on injected signals with an amplitude of  $H_0 = 2 \times 10^{-25}$ . This is in the middle of the range of the expected amplitude of a CW signal, so it would be insightful for this analysis to be repeated on injected signals with a lower limit amplitude of  $H_0 = 2 \times 10^{-27}$ .

In addition, the polarization parameters were kept constant for every injection used in the study. In future analysis, the polarization parameters should be changed for different injections, and explored in a grid, using the same exploration process as the frequency spin-down grids and the sky location grids in this study. While grids over sky location were used in this study, more analysis would need to be done with them in future work.

Finally, the most significant future work is to apply this analysis procedure to signal candidates from a directed search. This would need to be done after the previous 3 steps are completed, and are the work that this study is preparing for.

## ACKNOWLEDGMENTS

I would like to Dr. Ornella Piccinni for being an amazing mentor and teaching me so much this summer, and for hosting me both virtually and in person in Rome. In addition I'd like to thank Dr. Pia Astone for letting me use her office, and welcoming me into her research group. This project was done through the University of Florida International REU program, funded by NSF grants NSF PHY-1950830 and NSF PHY-1460803. Thank you to Dr. Paul Fulda and Dr. Peter Wass for organizing the program and the travel, and giving me the opportunity to do this research!

- 
- [1] P. Astone, S. D'Antonio, S. Frasca, and C. Palomba, A method for detection of known sources of continuous gravitational wave signals in non-stationary data, *Classical and Quantum Gravity* **27**, 194016 (2010).
- [2] O. J. Piccinni, P. Astone, S. D'Antonio, S. Frasca, G. Intini, P. Leaci, S. Mastrogiovanni, A. Miller, C. Palomba, and A. Singhal, A new data analysis framework for the search of continuous gravitational wave signals, *Classical and Quantum Gravity* **36**, 015008 (2019), arXiv:1811.04730 [gr-qc].
- [3] O. J. Piccinni, P. Astone, S. D'Antonio, S. Frasca, G. Intini, I. La Rosa, P. Leaci, S. Mastrogiovanni, A. Miller, and C. Palomba, Directed search for continuous gravitational-wave signals from the Galactic Center in the Advanced LIGO second observing run, *Phys. Rev. D* **101**, 082004 (2020), arXiv:1910.05097 [gr-qc].
- [4] P. Astone, A. Colla, S. D'Antonio, S. Frasca, and C. Palomba, Method for all-sky searches of continuous gravitational wave signals using the frequency-Hough transform, *Phys. Rev. D* **90**, 042002 (2014), arXiv:1407.8333 [astro-ph.IM].